

The Topological Susceptibility of the Lattice CP^{n-1} Model on the Torus and the Sphere ¹

N. Schultka ^{*}, M. Müller-Preussker ^{**}

** Department of Physics
The Florida State University
Tallahassee, FL 32306, USA*

*** Humboldt-Universität zu Berlin, Fachbereich Physik
Institut für Elementarteilchenphysik
Invalidenstr. 110, O-1040 Berlin, Germany*

Abstract

The topological vacuum structure of the two-dimensional CP^{n-1} model for $n = 3, 5, 7$ is studied on the lattice. In particular we investigate the small-volume limit on the torus as well as on the sphere and compare with continuum results. For $n \geq 5$, where lattice artifacts should be suppressed, the topological susceptibility shows unexpectedly strong deviations from asymptotic scaling. On the other hand there is an indication for a convergence to values obtained analytically within the limit $n \rightarrow \infty$.

¹This research project was partially funded by the Department of Energy under the contract DE-FG05-87ER40319

1. Introduction

The $2D$ CP^{n-1} model [1] is a convenient play-model for testing non-perturbative methods aimed for application in asymptotically free field theories like QCD. Because of the existence of classical (multi-) instanton solutions it allows a semi-classical treatment [2, 3]. It can be considered within approximations based on the $1/n$ expansion [4, 5] as well as within the lattice approach [6 - 14].

One of the main quantities calculated within these different approaches is the so-called topological susceptibility χ_t , i. e. the zero momentum correlator of the topological charge density. For quenched QCD the analogous quantity has an important physical meaning, since it is directly related to the mass of the η' meson (solution of the $U_A(1)$ problem [15]).

However, in computing χ_t one meets serious difficulties both in the continuum and on the lattice. In the continuum the semi-classical approach can be developed in a closed form only for the sectors of exact multi-(anti-) instanton amplitudes. The contribution of mixed instanton and antiinstanton configurations to the corresponding functional integral has to rely on model assumptions, like the dilute instanton gas or liquid models in QCD. Only in the small-volume limit, where the one-instanton contribution dominates, reliable results [16] were obtained consistent with those of an $1/n$ expansion [5]. Technically this achievement was possible by formulating the CP^{n-1} model on a sphere S^2 . (The same holds for the pure $SU(N_c)$ Yang-Mills theory treated on S^4 [17]). On the other hand, on the lattice there is the danger to encounter lattice artifacts, which were shown to spoil the continuum limit of the topological susceptibility at least for $n \leq 3$ [6, 7, 8]. The analogous problem occurs in pure $SU(2)$ lattice gauge theory when the geometric method to define the topological charge [18] is directly applied to the Monte Carlo generated quantum fluctuations of the gauge field [19].

All these difficulties so far have prevented a real consistency check between the continuum approaches and lattice computations. Since new techniques for updating the complex vector fields are available [22] we can study the lattice CP^{n-1} model for higher n , where lattice artifacts should be suppressed. Furthermore, we treat the model both on a torus and on a sphere. The latter case gives us the opportunity to investigate the topological structure in the small-volume limit with the same boundary conditions as it was done in the continuum case [16].

In our previous papers [10] we concentrated on the CP^3 model. We used a lattice formulation of the model, where the Abelian gauge field involved was considered as a dynamical one. We found a situation which bears a great resemblance to that in $SU(2)$ lattice gauge theory: With the geo-

metric method one finds an almost perfect asymptotic scaling behaviour for the topological susceptibility even on very small lattices, although there are dislocations expected to spoil the continuum limit. Thus, one is tempted to ask whether the scaling behaviour is accidental and could be disturbed if dislocations and other short range fluctuations are suppressed.

Here we come back to another lattice formulation first considered by Petcher and Lüscher [9] and apply to it the cluster updating algorithm [22, 12]. The cases $n = 3, 5, 7$ will be treated. We shall investigate the topological properties and estimate the correlation lengths ξ both for the two-dimensional torus T^2 and for the sphere S^2 . We are going to discuss the behaviour of the topological susceptibility down to volumes $V \simeq \xi^2$ and to compare our lattice results with those relying on the $1/n$ expansion.

Section 2 will collect all continuum results needed for our discussion. The lattice formulation on T^2 and S^2 , respectively, will be presented in Chapter 3. Section 4 is devoted to the Monte Carlo results. The conclusions will be drawn in Section 5.

2. The CP^{n-1} Model

The CP^{n-1} model on an arbitrarily curved two-dimensional manifold is defined by the following action [1]

$$S = \frac{n}{2f} \int d^2x \sqrt{g} g^{\mu\nu} D_\mu z_a \overline{D_\nu z_a}, \quad (1)$$

where $g^{\mu\nu}$ denotes the metric tensor. The complex vector field $z_a(x)$, $a = 1, \dots, n$ is subjected to the normalization condition

$$z_a \overline{z_a} = 1. \quad (2)$$

D_μ stands for the total covariant derivative, i.e. it consists of the derivative ∇_μ in a curved space and in our case a $U(1)$ gauge field A_μ ,

$$D_\mu = \nabla_\mu + iA_\mu. \quad (3)$$

∇_μ acts on an arbitrary vector B_μ in the curved space according to

$$\nabla_\mu B_\nu = \partial_\mu B_\nu - \Gamma_{\mu\nu}^\alpha B_\alpha, \quad (4)$$

where $\Gamma_{\mu\nu}^\alpha$ denote the Christoffel symbols.

Expressing the gauge field A_μ completely in terms of the z -field,

$$A_\mu = -\frac{i}{2} (z_a \partial_\mu \overline{z_a} - \overline{z_a} \partial_\mu z_a), \quad (5)$$

enables us to write

$$S = \frac{n}{2f} \int d^2x \sqrt{g} g^{\mu\nu} (\partial_\mu z \partial_\nu \bar{z} + (z \partial_\mu \bar{z})(z \partial_\nu \bar{z})) . \quad (6)$$

It is convenient to introduce projection matrices as follows [9]

$$P_{\alpha\beta}(x) = z_\alpha(x) \bar{z}_\beta(x) \quad (7)$$

satisfying

$$P = P^\dagger, \quad P^2 = P, \quad \text{Tr} P = 1 \quad \forall x . \quad (8)$$

Expressing (1) in terms of (7), we get

$$S = \frac{n}{4f} \int d^2x \sqrt{g} g^{\mu\nu} \text{Tr} [\partial_\mu P \partial_\nu P] . \quad (9)$$

For our model the topological charge Q can be defined as

$$\begin{aligned} Q &= \int d^2x \rho(x) , \\ \rho(x) &= \frac{1}{2\pi} \varepsilon_{\mu\nu} \nabla_\mu A_\nu , \end{aligned} \quad (10)$$

where $\varepsilon_{12} = -\varepsilon_{21} = 1$. This charge can be understood as the quantized "magnetic flux" through the surface. Expressing this "flux" in terms of the z -fields we get

$$Q = -\frac{i}{2\pi} \int d^2x \varepsilon_{\mu\nu} \partial_\mu z \partial_\nu \bar{z} . \quad (11)$$

The following relation connects the action (1) and the topological charge (10)

$$S \geq \frac{\pi n}{f} |Q| . \quad (12)$$

In case that (12) becomes an equality, we are led to the self-duality relation

$$D^\nu z = \mp \frac{i}{\sqrt{g}} \varepsilon_{\nu\alpha} D_\alpha z . \quad (13)$$

For the 2-dimensional flat infinite space the (multi-) instanton solutions of (13) look as follows [6]

$$\begin{aligned} z_\alpha &= \frac{p_\alpha(x)}{|p(x)|} , \\ p_\alpha &= C_\alpha \prod_{j=1}^Q (x_1 - ix_2 - a_\alpha^j) , \quad C_n = 1 . \end{aligned} \quad (14)$$

All the a_α^j are different from each other, and x_1, x_2 denote the coordinates in flat space. Note that the topological charge is determined by the zeros of the polynomials p_α . In the case of our manifold being the sphere S^2 the coordinates x_1, x_2 have to be understood as the stereographic coordinates.

The model is quantized using the functional integration method. Quantum expectation values of operators $O(z, \bar{z})$ have to be calculated as follows.

$$\langle O(z, \bar{z}) \rangle = Z^{-1} \int DzD\bar{z} O(z, \bar{z}) \exp(-S), \quad (15)$$

$$DzD\bar{z} = \prod_x \prod_{\alpha=1}^n \frac{dz_\alpha(x) d\bar{z}_\alpha(x)}{2\pi i}, \quad \delta \left(\sum_{\beta=1}^n z_\beta(x) \bar{z}_\beta(x) - 1 \right) \quad (16)$$

with $Z = \int DzD\bar{z} \exp(-S)$. The observables we are really interested in throughout this paper are the topological susceptibility χ_t and the correlation length ξ . The latter can be read off from the long-distance behaviour (cf. the next paragraph) of the correlation function

$$\begin{aligned} C(x, y) &= \left\langle \left| \sum_\alpha z_\alpha(x) \bar{z}_\alpha(y) \right|^2 \right\rangle - \sum_{\alpha, \beta} \langle z_\alpha(x) \bar{z}_\beta(y) \rangle \langle z_\beta(y) \bar{z}_\alpha(x) \rangle \\ &= \left\langle \left| \sum_\alpha z_\alpha(x) \bar{z}_\alpha(y) \right|^2 \right\rangle - \frac{1}{n} \end{aligned} \quad (17)$$

The topological susceptibility is defined as follows.

$$\chi_t = \int d^2x \langle \rho(x) \rho(0) \rangle = \frac{\langle Q^2 \rangle}{V}, \quad (18)$$

where V is the "volume" (i. e. the surface area) of the manifold under consideration (either the sphere S^2 or the torus T^2). χ_t can be rewritten as

$$\chi_t = \frac{1}{V} \sum_{Q=-\infty}^{Q=\infty} Q^2 P_Q, \quad (19)$$

with P_Q the probability for a field configuration to have the topological charge Q . On the sphere S^2 this formula can actually be exploited within the limit of a small volume [16] where it gives

$$\chi_t \simeq \frac{2}{V} P_1, \quad (20)$$

i.e., only the one-(anti-) instanton contribution turns out to be dominant. The result is

$$\chi_t(V) \Lambda_{MS}^{-2} = \frac{2C_1(n)}{V \Lambda_{MS}^2} \left[- \left(\frac{V \Lambda_{MS}^2}{4\pi} \right)^{\frac{1}{2}} \frac{n}{\pi} \ln \frac{V \Lambda_{MS}^2}{4\pi} \right]^n. \quad (21)$$

The coefficients $C_1(n)$ are numerically known, in particular

$$\begin{aligned} C_1(3) &= 27.264 \\ C_1(5) &= 3.963 \\ C_1(7) &= 0.343 . \end{aligned} \tag{22}$$

On the other hand, the model is $1/n$ -expandable [4]. The result within the leading order and for $V = \infty$ is

$$\chi_t(\infty) = \frac{3}{4\pi n \xi^2} + O\left(\frac{1}{n^2}\right), \tag{23}$$

where ξ denotes the correlation length, which tends to a finite large n limit

$$\xi \Lambda_{MS} = \frac{1}{4\sqrt{\pi}} e^{-\frac{1}{2}\Gamma'(1)} = 0.188 . \tag{24}$$

On the contrary, if the model is treated within the $1/n$ expansion on a sphere S^2 having a small finite surface area V , then $\chi_t(V)$ behaves in accordance with the semi-classical result (21) [5]. The limits $n \rightarrow \infty$ and $V \rightarrow \infty$ do not commute.

It is worthwhile for our further considerations to replace Λ_{MS} in (21) by ξ obtained at $V = \infty$ (24).

$$\chi_t(V)\xi^2 = \frac{2C_1(n)}{V\xi^{-2}} \left[- \left(\frac{V}{4\pi} \left(\frac{0.188}{\xi} \right)^2 \right)^{\frac{1}{2}} \frac{n}{\pi} \ln \frac{V}{4\pi} \left(\frac{0.188}{\xi} \right)^2 \right]^n \tag{25}$$

3. The Lattice Formulation

First, let us describe the lattice constructions for the torus and the sphere. We decided to use simplicial lattices as the most convenient way for discretizing curved manifolds. In the torus case it will allow us directly to compare with [9] and, as we shall explain below, with $1/n$ expansion results.

Torus T^2 : The plaquettes of the lattice are equilateral triangles with edge length a . A lattice point \vec{x} is then described by

$$\vec{x} = x_1 \vec{n}_1 + x_2 \vec{n}_2$$

where

$$\vec{n}_1 = a(1, 0), \quad (26)$$

$$\vec{n}_2 = a\left(\frac{1}{2}, \frac{\sqrt{3}}{2}\right) \quad (27)$$

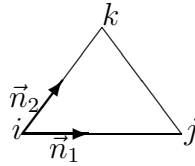
The topology of the torus is established by imposing periodic boundary conditions on the functions defined on the lattice.

$$f(\vec{x} + N_1\vec{n}_1 + N_2(\vec{n}_2 - \vec{n}_1)) = f(\vec{x}) \quad (28)$$

where N_1 and $N_2/2$ are integers. The surface area V of the torus is

$$V = \frac{\sqrt{3}}{2}N_1N_2a^2.$$

Sphere S^2 : The sphere S^2 is discretized by a simplicial lattice in the following way. We start from a regular tetrahedron with corners placed at the surface of the sphere. Then we make several *steps of refinement* of this initial lattice. During each step we project the center of each given link onto the surface to introduce further sites. All sites, the old and new ones, are connected with their nearest neighbours by straight lines. After each step every simplex is replaced by four new simplices. After N steps we have $P = 2(4^N + 1)$ sites and $L = 3(P - 2)$ links. Figs. 1, 2 show subsequent steps of refinement and the obtained link length distribution, respectively. In order to define a metric on these lattices, we consider the triangles to be flat. Identifying one of the corners i with the origin of the local coordinate system, we have for the triangle (i,j,k) [23]



the following metric tensor

$$g^{\mu\nu} = \frac{l_1^2 l_2^2}{4\Delta^2} M^{\mu\nu}$$

$$M = \begin{pmatrix} 1 & -\vec{n}_1\vec{n}_2 \\ -\vec{n}_1\vec{n}_2 & 1 \end{pmatrix}, \quad (29)$$

where Δ is the area of the triangle and l_i are the lengths of the links corresponding to the unit vectors \vec{n}_i .

Lattice action: The most convenient way to discretize the lattice action uses its representation in terms of the projection matrices (9). Thus we have

$$S = \frac{n}{4f} \sum_{\Delta} \Delta g^{\mu\nu} \text{Tr} [\partial_{\mu} P \partial_{\nu} P] , \quad (30)$$

where the partial derivative has to be taken as follows:

$$\partial_{\mu} P = \frac{P(x + l_{\mu} \vec{n}_{\mu}) - P(x)}{l_{\mu}} \quad \mu = 1, 2 . \quad (31)$$

(30) can be rewritten as a sum over links $\langle ij \rangle$ between nearest neighbour sites i, j

$$S = \beta \sum_{\langle ij \rangle} S_{ij} \quad , \quad \beta = \frac{n}{4f} \quad (32)$$

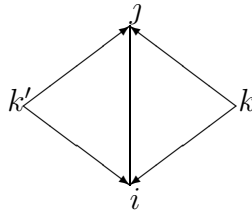
with

$$S_{ij} = \Gamma_{ij} \left(1 - |z(i)\bar{z}(j)|^2 \right) \quad (33)$$

and the weight factors

$$\Gamma_{ij} = \frac{\vec{l}_{kj} \vec{l}_{ki}}{2 \Delta(i, j, k)} + \frac{\vec{l}_{k'j} \vec{l}_{k'i}}{2 \Delta(i, j, k')} . \quad (34)$$

The corresponding geometry is shown in the figure.



The action (32) is obviously $U(1)$ gauge invariant. Note that in the case of the torus T^2 the weights are constant:

$$\Gamma_{ij} = \frac{2}{\sqrt{3}} , \quad (35)$$

i.e., we obtain the action invented in [9].

Topological charge: For a given field configuration on the lattice, the topological charge is computed by using its definition according to [9].

$$Q = \sum_{\Delta} q(\Delta) \quad q(\Delta) \in \left(-\frac{1}{2}, \frac{1}{2} \right) , \quad (36)$$

where

$$\exp(i2\pi q(\Delta)) = \frac{\text{Tr} (P(k)P(j)P(i))}{|\text{Tr}(P(k)P(j)P(i))|} . \quad (37)$$

The sum runs over all (positively oriented) triangles. Equation (37) rewritten in terms of the z -field means

$$\exp(i2\pi q(\Delta)) = \frac{z(i)\bar{z}(j)}{|z(i)\bar{z}(j)|} \frac{z(j)\bar{z}(k)}{|z(j)\bar{z}(k)|} \frac{z(k)\bar{z}(i)}{|z(k)\bar{z}(i)|} \quad (38)$$

$$= \exp(i(\phi(i, j) + \phi(j, k) + \phi(k, i))) \quad (39)$$

and finally

$$2\pi q(\Delta) = \phi(i, j) + \phi(j, k) + \phi(k, i) + 2\pi m(\Delta) \quad \epsilon(-\pi, \pi], \quad (40)$$

with $m(\Delta)$ a properly chosen integer.

Monte Carlo simulation: The expectation values (15) are computed numerically using the Monte Carlo method. We generate equilibrium field configurations by applying the one-cluster algorithm invented by U.Wolff [22]. This algorithm can be easily implemented for arbitrary n and works reasonably fast, in spite of the fact that it does not remove critical slowing down [12]. We choose an arbitrary lattice site x_0 and collect adjacent lattice points into the cluster with the bond probability

$$p = (1 - \exp(-\beta\Delta S_{ij})) \theta(\Delta S_{ij}) , \quad (41)$$

$$\Delta S_{ij} = S_{ij} (R z(i), z(j)) - S_{ij} (z(i), z(j)) , \quad (42)$$

with S_{ij} the link action (33) and

$$\theta(\Delta S_{ij}) = \begin{cases} 1 & \text{for } \Delta S_{ij} > 0 \\ 0 & \text{otherwise} \end{cases} \quad (43)$$

Having found all sites belonging to the cluster, the field vectors sitting at these sites are flipped. The flip operation R acting on the fields z is defined as follows:

$$R z = z - 2(\bar{r}z)r, \quad (44)$$

where r is a random vector in the z -space, i.e.,

$$\sum_{\alpha=1}^n r_{\alpha} \bar{r}_{\alpha} = 1. \quad (45)$$

Note that

$$R^2 z = z , \quad (46)$$

$$(Rz(i))\overline{(Rz(j))} = z(i)\overline{z(j)}. \quad (47)$$

Choosing the bond probability and the flip operation as above endows the algorithm with detailed balance [22, 25]. Fig. 3 shows the cluster point distribution for the CP^6 Model on the torus T^2 with $\beta = 4.6$ on a 100×100 lattice. The average number of cluster points is 6516.

In order to test the reliability of our program we compared the expectation value of the link action (33) with analytical results. On the torus, the following weak coupling formula holds [9]

$$\beta \gg 1 \quad \langle S_{ij} \rangle = \frac{2}{3} \left(\frac{n-1}{2} \frac{1}{\beta} + \frac{(n-1)n}{16\sqrt{3}} \frac{1}{\beta^2} + \dots \right) \quad (48)$$

and for $\beta = 0$ the strong coupling ones

$$\langle S_{ij} \rangle = \frac{2}{\sqrt{3}} \frac{n-1}{n} \quad \text{on the torus } T^2, \quad (49)$$

$$\langle S_{ij} \rangle = \bar{\Gamma}_{ij} \frac{n-1}{n} \quad \text{on the sphere } S^2, \text{ where} \quad (50)$$

$$\bar{\Gamma}_{ij} = \frac{1}{L} \sum_{ij} \Gamma_{ij} \quad \text{with } L \text{ the number of links.}$$

Fig. 4 shows the analytical curve (48) compared with our numerical values for S_{ij} versus β for the CP^2 and CP^4 Model on the torus T^2 . For $\beta = 0$, we found

	$\langle S_{ij} \rangle$	
	Analytic ((49) resp. (50))	Numeric
torus T^2		
CP^2 Model	.7698	.7701
CP^4 Model	.9238	.9231
sphere S^2		
$\bar{\Gamma}_{ij} = 1.5416$ ($N = 3$)		
CP^2 Model	1.0277	1.0266
CP^4 Model	1.2333	1.2318

The purely statistical errors are omitted because they were found of order 10^{-5} .

In order to compute the correlation function, we used the *improved estimator method* [24, 12], i.e.,

$$C(x) = (n+1) \left\langle \frac{P}{|c|} \theta(x, c) \theta(0, c) \text{Re} \left[(\bar{z}(x)z(0) - (\bar{z}(x)r)(\bar{r}z(0))) \overline{(\bar{z}(x)r)(\bar{r}z(0))} \right] \right\rangle \quad (51)$$

where r denotes the reflexion vector (44) and

$$\theta(x, c) = \begin{cases} 1 & \text{if } x \text{ belongs to the cluster} \\ 0 & \text{otherwise.} \end{cases} \quad (52)$$

P and $|c|$ are the number of all lattice points and the number of all cluster points respectively.

Correlation lengths: ξ is extracted as follows.

Torus T^2 : Representing the point x as $\vec{x} = x_1\vec{n}_1 + x_2(\vec{n}_2 - \vec{n}_1)$ and using the vectors \vec{n}_1 and \vec{n}_2 from (26) and (27), we actually compute

$$\tilde{C}(x_2) = \sum_{x_1=0}^{l_1-1} C(x_1, x_2). \quad (53)$$

In the range $0 \ll x_2 \ll l_2$, we expect the following behaviour

$$\tilde{C}(x_2) = A \cosh \frac{x_2 - \frac{l_2}{2}}{\xi}, \quad (54)$$

where the constant A and the correlation length ξ are extracted by fitting the Monte Carlo data.

Sphere S^2 : In order to find the shape of the correlation function we start from a free, scalar, massive, Euclidean theory on the sphere S^2 . The propagator is as usual

$$G = \frac{1}{\Delta + m^2}, \quad (55)$$

$$\Delta = -\frac{1}{\sqrt{g}}\partial_\mu(\sqrt{g}\partial^\mu). \quad (56)$$

Using spherical coordinates, the following equation has to be solved:

$$\left(-\frac{1}{R^2}\frac{1}{\sin^2\vartheta}\partial_\varphi^2 - \frac{1}{R^2\sin\vartheta}\partial_\vartheta(\sin\vartheta\partial_\vartheta) + m^2\right)G(\varphi, \vartheta, \varphi', \vartheta') = \delta(\varphi, \vartheta, \varphi', \vartheta') \quad (57)$$

or

$$\left(-\frac{1}{\sin^2\vartheta}\partial_\varphi^2 - \frac{1}{\sin\vartheta}\partial_\vartheta(\sin\vartheta\partial_\vartheta) + (mR)^2\right)G(\varphi, \vartheta, \varphi', \vartheta') = \sum_{l,m} Y_{l,m}(\varphi, \vartheta)\bar{Y}_{l,m}(\varphi', \vartheta'), \quad (58)$$

where the bar means complex conjugation. Thus,

$$G(\varphi, \vartheta, \varphi', \vartheta') = \frac{1}{4\pi} \sum_{l=0}^{\infty} \frac{2l+1}{l(l+1) + (mR)^2} P_l(\cos \tilde{\vartheta}), \quad (59)$$

where $\tilde{\vartheta} \in [0, \pi]$ denotes the angle between the points (φ, ϑ) and (φ', ϑ') . We fitted the Monte Carlo data according to

$$C(\vartheta(x), 0) = A \sum_{l=0}^{l_{max}} \frac{2l+1}{l(l+1) + \left(\frac{R}{\xi}\right)^2} P_l(\cos \vartheta) \quad (60)$$

in the range $0 \ll \vartheta(x) \leq \pi$, truncating the series at $l_{max} = 100$, which provides stable results.

Scaling: Physical observables, e. g. $\chi_t = \langle Q^2 \rangle / V$ and ξ , are measured in units of the average link length \bar{l} , which is related to β through the 2-loop renormalization group expression [9]

$$\Lambda_L \bar{l} = \left(\frac{4\pi}{n} \beta \right)^{\frac{2}{n}} e^{-\frac{4\pi}{n} \beta}. \quad (61)$$

Then, approaching the continuum limit $\chi_t \bar{l}^2$ and $\xi \bar{l}^{-1}$ are expected to behave like

$$\xi \bar{l}^{-1} = C_\xi \left(\frac{4\pi}{n} \beta \right)^{-\frac{2}{n}} e^{\frac{4\pi}{n} \beta} \quad (62)$$

$$\chi_t \bar{l}^2 = C_\chi \left(\frac{4\pi}{n} \beta \right)^{\frac{4}{n}} e^{-\frac{8\pi}{n} \beta} \quad (63)$$

(On T^2 replace \bar{l} by the lattice spacing a .)

We have checked the occurrence of dislocations (i.e. lattice fields z_α that have a topological charge $Q = \pm 1$ with respect to definition (36), (37) but have an action below $8\pi\beta/n$ i. e. the scaling exponent of $\chi_t \bar{l}^2$) by minimizing the action of the CP^1 model while keeping the topological charge fixed. We have found

	S_d
sphere S^2	$2.09\pi\beta$
torus T^2	$2.06\pi\beta$

For higher values n the CP^1 configurations can be simply embedded. Therefore the dislocations found become suppressed for sufficiently large β at $n \geq 4$.

Let us consider the lattice CP^{n-1} Model for large n on the torus T^2 . Then (61) enables us to find the curve that ξa^{-1} and $\chi_t a^2$ should lie on if we approach the infinite volume limit. Equations (23) and (24) provide us with

$$\chi_t(\infty)a^2 = \frac{12}{n} e^{\Gamma(1)} (a\Lambda_L)^2 \left(\frac{\Lambda_{MS}}{\Lambda_L} \right)^2. \quad (64)$$

Introducing (61) and

$$\frac{\Lambda_{MS}}{\Lambda_L} = 2\sqrt{3} \exp \left(-\frac{1}{2}(\ln \pi + \Gamma'(1)) + \frac{\pi}{\sqrt{3}} \right) \quad (65)$$

[9] into (64) gives $\chi_t(\infty)a^2$. For $n \geq 4$ we expect our data to approach this curve for increasing n and $\xi \gg a$. For the correlation length, we get

$$\xi a^{-1} = \frac{1}{4\sqrt{\pi}} e^{-\frac{1}{2}\Gamma'(1)} \frac{1}{a\Lambda_L} \frac{\Lambda_L}{\Lambda_{MS}}. \quad (66)$$

4. Results

We have simulated the CP^{n-1} model with $n = 3, 5,$ and 7 , each case at a variety of β values and lattice sizes up to 10^2 and 60×120 , respectively, for T^2 and up to division $N = 6$ for S^2 . Typically we carried out 10^4 cluster updates for thermalization followed by $O(10^3)$ ($O(10^4)$) measurements of the topological charge (correlation function) separated by 10 (5) cluster updates. A cluster update means building up one cluster and flipping all the z 's within this cluster.

Figs. 5 - 9 show our main data. The errors of the topological susceptibility indicated were estimated by collecting the measured values into groups of $O(100)$ single measurements and by taking the statistical error of the group averages. In order to determine the correlation length we splitted our data for the correlation function into 5 groups. For each of them we fitted the correlation length separately and estimated the error from these values.

In Figs. 5 we show the topological susceptibility for the cases $n = 3, 5,$ and 7 on T^2 as a function of the " n -invariant" coupling $f^{-1} = 4\pi\beta/n$. The approximate scaling behaviour or weak scaling violation seen for CP^2 (Fig. 5a) is in accordance with the observations in [9] and is related to the dominance of dislocations. In fact, at larger f^{-1} values the Monte Carlo time-histories for the topological charges have shown us the dominance of short-range fluctuations (i. e. only very short appearance of charges being unequal to zero).

For the cases CP^4 and CP^6 , where dislocations become definitely suppressed, we see a surprisingly strong deviation from asymptotic scaling in the opposite direction. This is in contrast to the conclusions drawn in [12] and in agreement with those of [14]. The investigation in [12] concentrated on data produced in a smaller f^{-1} -range. Thus the falling tail at smaller bare coupling was missed. Nevertheless, the data presented there (with another lattice discretization) are compatible with ours. The time histories of topological charges show freezing effects within sectors of non-vanishing Q over a few hundreds of consecutive charge measurements. This means long-range topological fluctuations occur. In spite of this, within the given β - or f^{-1} - range the cluster algorithm allows for sufficient tunneling between the sectors such that we consider our results for the topological susceptibility reliable up to the largest f^{-1} -values shown.

In Figs. 5b,c, for comparison, we have drawn also the leading $1/n$ result for $\chi_t(\infty)$ according to (64). There seems to be a tendency to reach the $1/n$ and continuum limit at very large β !

Figs. 6 present the analogous data for the case of the sphere S^2 . The observations and conclusions concerning the scaling violation are definitely the same. The $1/n$ limit cannot be given here because of the unknown Λ -ratio (compare with (65)). The comparison of Figs. 5 with Figs. 6 shows stronger finite-size effects in the S^2 -case than for the torus T^2 .

In order to study the behaviour of the topological susceptibility as a function of the physical volume we measured the correlation length ξ . Figs. 7, 8 show the results of our fits to the correlation functions as described above and represented as functions of f^{-1} . Figs. 7a, b present the cases CP^4 and CP^6 on T^2 , whereas Fig. 8 shows CP^6 on S^2 . All these data obtained for the correlation length are compatible with asymptotic scaling or even with slight scaling violations as reported in [14]. About possible convergence to the $1/n$ -limit we cannot draw here any conclusion. We need better statistics by at least one order of magnitude or/and an improved cluster, overrelaxation or multigrid algorithm [14].

Finally, in Fig. 9 we study the volume dependence of the topological susceptibility for $n = 7$ and S^2 taking χ_t and the volume V (surface area of S^2) in units of the correlation length ξ , which itself corresponds to the infinite-volume limit. The big error bars are due to the statistical errors of ξ . Nevertheless, we see the expected tendency of a suppression of topological fluctuations in the limit of a small volume V . Fig. 9 contains the analytic result (25), too, represented by a continuous line. Thus, we are qualitatively in the right ball park. But a real quantitative comparison with the continuum behaviour below $V \simeq \xi^2$ needs yet large efforts in future.

5. Conclusions

In this paper we have studied the topological properties of the $2D$ CP^{n-1} model on a lattice for varying n and for the cases of a (flat) torus and a sphere. We used the cluster update algorithm which can be economically implemented, and which allows to treat larger n 's and larger lattice sizes at intermediate coupling values than the standard Metropolis algorithm. We convinced ourselves that there is a reasonable tunneling rate between different topological sectors with long-living, large-scale field configurations in the coupling range considered. This does not mean that the algorithm allows to suppress critical slowing down. The contrary was shown in [12].

The main quantity considered was the topological susceptibility. It shows a strong violation effect from asymptotic scaling for $n \geq 5$ on T^2 as well as on S^2 . In this case dislocations are known to become suppressed for sufficiently large β . On the other hand for $n = 3$ we recovered approximate scaling or slight scaling violation into the opposite direction due to the presence of dislocations.

We compared the outcome of the Monte Carlo investigation with the analytical leading order $1/n$ result for infinite volume. Our data provide an indication that for very large β the $1/n$ result combined with asymptotic scaling could be reached.

Unfortunately, within the given statistics the improved estimator method did not provide us correlation lengths ξ for large volumina with sufficient high accuracy in order to study the limit of small volume $V \rightarrow 0$ in terms of physical units ξ . So the comparison of the semi-classical and $1/n$ behaviour on the sphere S^2 in this limit deserves further investigations. So far we obtained qualitatively a reasonable behaviour at $V \geq \xi^2$. The multigrid method can provide a possibility to improve that. We hope to come back to this question very soon.

Acknowledgements

We would like to thank M. Lüscher, U.-J. Wiese for valueable discussions. Also one of us (M.M.-P.) would like to express his deep gratitude to all colleagues at Bielefeld University for the kind hospitality extended to him. We are indebted to M. Hasenbusch and St. Meyer for sending us their data for CP^3 prior to publication.

References

- [1] H. Eichenherr, Nucl. Phys. **B146** (1978) 215;
V. L. Golo, A. M. Perelomov, Phys. Lett. **79B** (1978) 112.
- [2] B. Berg, M. Lüscher, Commun. Math. Phys. **69** (1979) 57.
- [3] J.-L. Richard, A. Rouet, Nucl. Phys. **B211** (1983) 447;
J.-L. Richard, Phys. Lett. **128B** (1983) 213;
V. A. Fateev, I. V. Frolov, A. S. Schwarz, Nucl. Phys. **B154** (1979) 1.
- [4] A. D'Adda, M. Lüscher, P. Di Vecchia, Nucl. Phys. **B146** (1978) 63;
M. Campostrini, P. Rossi, Pisa University preprint IFUP-TH 91-33.
- [5] G. Münster, Phys. Lett. **118B** (1982) 380; Nucl. Phys. **B218** (1983) 1.
- [6] B. Berg, M. Lüscher, Nucl. Phys. **B190** [FS3] (1981) 412.
- [7] M. Lüscher, Nucl. Phys. **B200** [FS4] (1982) 61.
- [8] B. Berg, Phys. Lett. **104BB** (1981) 475.
- [9] D. Petcher, M. Lüscher, Nucl. Phys. **B225** [FS9] (1983) 53.
- [10] B. Jozefini, M. Müller-Preussker, N. Schultka, Phys. Lett. **234B** (1990) 329;
B. Jozefini, M. Müller-Preussker, N. Schultka, H. Stüben, Proceedings XXIV Int. Symp. Ahrenshoop, Gosen, p. 299 (1991); Z. Phys. **C-Particles and Fields** **51** (1991) 491.
- [11] H. Stüben, H.-C. Hege, A. Nakamura, Phys. Lett. **244B** (1990) 473.
- [12] K. Jansen, U.-J. Wiese, Nucl. Phys. **B370** (1992) 762.
- [13] A. C. Irving, C. Michael, Nucl. Phys. **B371** (1992) 521.
- [14] M. Hasenbusch, S. Meyer, Kaiserslautern preprints Th 91-16 (1991), Th 91-23 (1991).
- [15] E. Witten, Nucl. Phys. **B156** (1979) 269;
G. Veneziano, Nucl. Phys. **B159** (1979) 213.
- [16] P. Schwab, Phys. Lett. **118B** (1982) 373; Phys. Lett. **126B** (1983) 241.
- [17] M. Lüscher, Nucl. Phys. **B205** [FS5] (1982) 483.

- [18] M. Lüscher, Commun. Math. Phys. **85** (1982) 29; A. Phillips, D. Stone, Commun. Math. Phys. **103** (1986) 599.
- [19] D.J.R. Pugh, M. Teper, Phys. Lett. **218B** (1989) 326; Phys. Lett. **224B** (1989) 159;
M. Göckeler et al., Phys. Lett. **233B** (1989) 192;
V.G. Bornyakov, B. Jozefini, M. Müller-Preussker, A.M. Zadorozhny, Dubna preprint E2-89-606 (1989).
- [20] M. Kremer et al., Nucl. Phys. **B305** (1988) 109.
- [21] R. H. Swendsen, J.-S. Wang, Phys. Rev. Lett. **58** (1987) 86.
- [22] U. Wolff, Phys. Rev. Lett. **62** (1989) 361.
- [23] M. Bander, C. Itzykson, Nucl. Phys. **B257** [FS14] (1985) 531.
- [24] U. Wolff, Nucl. Phys. B (Proc. Suppl.) 17 (1990) 93.
- [25] K. Binder, Applications of the Monte Carlo method in statistical Physics, Heidelberg u.a.: Springer 1984.

Figure captions

Fig. 1: First three steps of refinement for discretizing the sphere S^2 .

Fig. 2: Link length distribution on S^2 for refinement step $N = 5$. Average link length is $\bar{l} = .08794$ for a unit sphere.

Fig. 3: Distribution of cluster sizes produced with the one-cluster algorithm [22] for T^2 with lattice size 100×100 and CP^6 at $\beta = 4.6$. The average size is 6516.

Fig. 4: Comparison of numerical $\langle S_{ij} \rangle$ values with analytic ones (continuous lines) at weak coupling. Squares (triangles) correspond to CP^2 (CP^4).

Fig. 5: Topological susceptibility as a function of f^{-1} for the torus T^2 and CP^2 (a), CP^4 (b) and CP^6 (c), respectively. The straight line corresponds to an asymptotic scaling behaviour. The dashed line is the $1/n$ result according to (64).

Fig. 6: Topological susceptibility as a function of f^{-1} for the sphere S^2 and CP^2 (a), CP^4 (b) and CP^6 (c), respectively. The straight line corresponds to asymptotic scaling.

Fig. 7: Correlation length ξ as a function of f^{-1} for T^2 and CP^4 (a) and CP^6 (b), respectively. Straight and dashed lines as in Figs. 5.

Fig. 8: Correlation length ξ as a function of f^{-1} for S^2 and CP^6 .

Fig. 9: Topological susceptibility as a function of the physical volume, both expressed in units of the correlation length. The continuous line shows the one-instanton result (25) acc. to [16]. The dashed line indicates the infinite volume $1/n$ result, cf. Eq. (23).